Combined Two-phase Co-flow and Counter-flow in a Gas Channel/ Porous Transport Layer Assembly

Beale, S. B.; Andersson, M.; Weber, N.; Marschall, H.; Lehnert, W.;

Originally published:

October 2020

ECS Transactions 98(2020)9, 305-315

DOI: https://doi.org/10.1149/09809.0305ecst

Combined Two-phase Co-flow and Counter-flow in a Gas Channel/Porous Transport Layer Assembly

S. B. Beale[a,b], M. Andersson[c], N. Weber[d], H. Marschall[e], and W. Lehnert[a,f]

[a] Forschungszentrum Jülich GmbH, 52425 Jülich, Germany
[b] Department of Mechanical and Materials Engineering, Queen's University, Kingston ON K7L, 3N6, Canada
[c] Department of Energy Sciences, Lund University, 22100 Lund, Sweden
[d] Institut für Fluiddynamik, Helmholtz-Zentrum Dresden-Rossendorf e.V., 01328 Dresden
[e] Center of Smart Interfaces, Technische Universität Darmstadt, Alarich-Weiss Straße 10, 64287 Darmstadt, Germany
[f] RWTH Aachen University, Aachen 52056, Germany

This paper considers a detailed numerical analysis of combined liquid-gas co-flow in a gas channel with liquid-gas counter-flow in a porous transport layer, obtained by digital reconstruction of nano-computer tomography images. From this, the domain is tessellated with an unstructured castellated (octree) mesh, upon which the equations of mass and momentum are solved by means of a volume-of-fluid method. Liquid water is introduced from an electrode where gaseous oxygen is simultaneously removed by electrochemical reduction; the resulting liquid-gas counter flow in the porous transport layer results in liquid droplets being entrained in co-flow in the gas channels and convected downstream.

Introduction

Both water electrolyzers and fuel cells, based on polymer electrolyte membrane technology are the subject of much attention, at present. Numerical analysis of electrochemical processes and devices has, together with analytical and experimental work, formed a cornerstone for applied research and development. Until recently, detailed analysis of two-phase flow phenomena has proved difficult or impossible to realize, due to limitations in computational resources. Calculations for multi-phase flow phenomena may be performed, for example using popular Eulerian-Eulerian [1, 2] and Eulerian-Lagrangian [3] approaches, typically based on additional closure assumptions. Wang and Cheng [4, 5] considered a so-called mixture model to describe the motion of a mixture of two phases in the porous layers of a polymer electrolyte fuel cell (PEFC), whereas Gurau et al. [6] solved the PEFC problem with an Eulerian-Eulerian methodology similar to those developed previously by Lo and Spalding [7]. Although, theoretically, such approaches can distinguish between two or more phases; in practice the phase boundaries become smeared due to volume-averaging and numerical diffusion, and each computational cell has volume fraction for phase i, α_i, such that $0 \leq \alpha_i \leq 1$ without any precise knowledge of the distribution of i within the cell. Conversely, in volume-of-fluid (VOF) methods, front-tracking is employed to distinguish between two immiscible phases. Le and Zhou [8] employed a commercial code to perform two-phase calculations in the serpentine passages

of a PFC. Andersson et al. [9-12] modeled droplet dynamics in PEFC gas channels under various conditions of static and dynamic contact angles with experimental validation. Niblett et al. [13] considered water drainage through the both ordered and random porous transport layers (PTLs) and subsequent entrainment by the gas in the channel of a PEFC.

Problem Statement

Geometry and mesh construction

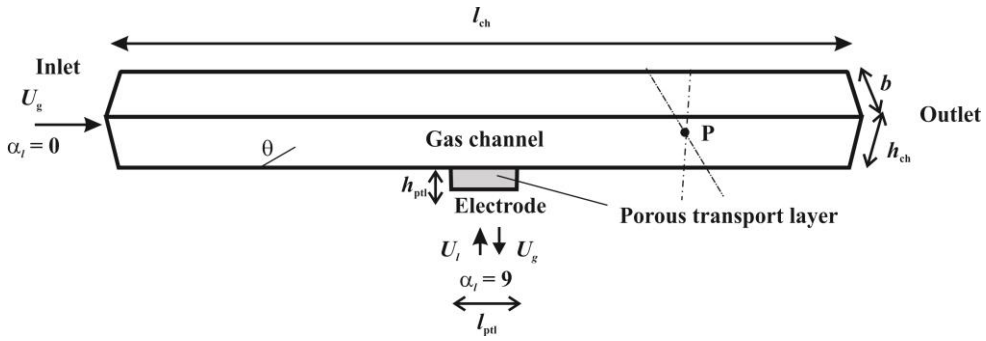

Figure 1. Schematic of problem under consideration.

The geometry considered is in the form of a 'T-shape' with the porous transport layer (PTL) in the form of a thin rectangular prism of dimensions 0.5×0.5×0.1 mm^3 located at the base of the 'T', and the gas flowing across the top in the channel, in the *x*-direction, as shown in Fig. 1. TABLE I provides details of the geometry considered. The PTL is reproduced by digital reconstruction of nano-computer tomography images of a Freudenberg H2315 PTL in the form of a stereolithography file, see Fig. 222(a). From this, the domain is tessellated with an unstructured castellated, or octree, type mesh, Fig. 2 (b). The open source software snappyHexMesh was employed. A mesh of 7.78×10^6 elements was constructed for the work described in this paper.

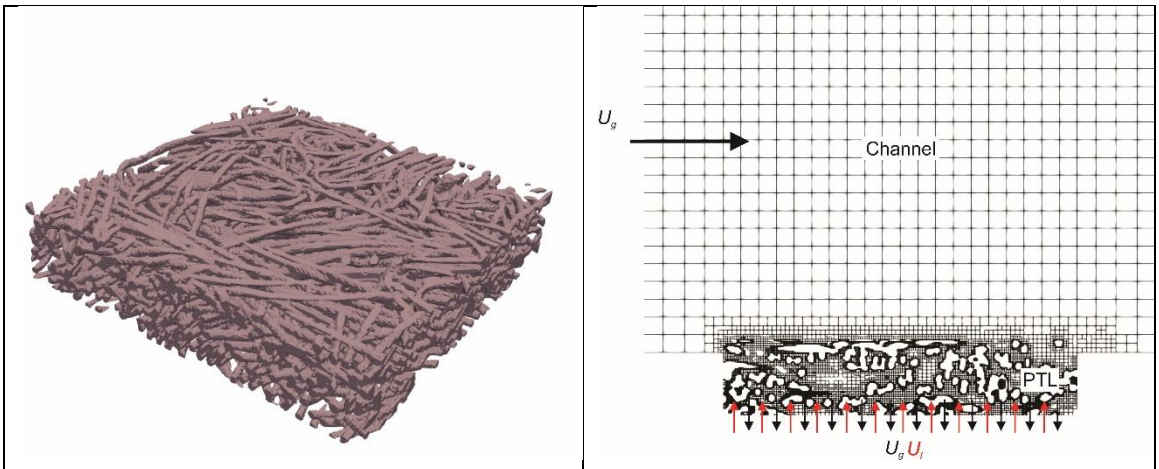

Figure 2. (a) Detail of a digitally reconstructed Freudenberg H2315 porous transport layer (b) two-dimensional slice of the castellated mesh, showing both channel and porous transport layer regions in a centre-plane corresponding to the main flow direction.

Volume-of-fluid method

The VOF method is applied to the problem-at-hand. It is assumed that the liquid phase is water, H_2O, and that the gas phase is pure oxygen, O_2. (N.B: The latter assumption may be relaxed to allow for injection/removal of pure oxygen to/from atmospheric air, in the future.) It is assumed that oxygen is consumed and liquid water produced at the cathode surface (oxygen electrode), in the *y*-direction. Figure 1 is a schematic of the problem at hand. In the VOF method, the mixture density is just:

$$\rho = \alpha_l \rho_l + \alpha_g \rho_g \tag{1}$$

and the mixture velocity is:

$$\boldsymbol{U} = \frac{\alpha_l \rho_l \boldsymbol{U}_l + \alpha_g \rho_g \boldsymbol{U}_g}{\rho} \tag{2}$$

Front tracking is expedited by solving an additional convection equation for α. A number of schemes (algebraic, geometric, etc.) have been described in the literature. In this study the multidimensional universal limiter with explicit solution (MULES) scheme was employed.

Boundary and initial conditions

TABLE I. Geometry.

Dimension	Length (mm)
l_{ch}	4.5
$l_{ch,i}$	2.0
$l_{ch,o}$	2.0
h_{ch}	0.5
b	0.5
l_{ptl}	0.5
h_{ptl}	0.1

TABLE II. Fluid properties

Symbol	Value
ρ_l	983 kg/m^3
ν_l	0.475×10^{-6} m^2/s
ρ_g	1.06 kg/m^3
ν_g	1.89×10^{-5} m^2/s

At the inlet, pure gas is injected with U = 10 m/s and α_l = 0. It is presumed that at the PTL/electrode boundary, liquid water is produced and oxygen is consumed. The effects of osmotic drag and membrane diffusion are not considered here, i.e., water is produced by the reaction only. Under the circumstances the net (mixture) mass flux is that due to hydrogen protons and electrons, namely;

$$\dot{m}_{H_2} = 9\dot{m}_{H_2O} - 8\dot{m}_{O_2} \tag{3}$$

The choice of $\alpha_l = 9$ and $\alpha_g = 1 - \alpha_l = -8$, renders the correct value of U in Eq. (3) while satisfying the requirement $\alpha_l + \alpha_g = 1$. It is to be noted that this is a boundary value for α_l, not an interior value, where $0 \le \alpha_l \le 1$ and $0 \le \alpha_g \le 1$ must strictly hold, at all times. The prescription is to be considered a purely numerical formulation for a counter-flow rather than a co-flow boundary condition, which would always result from $0 \le \alpha_l \le 1$ values. This distinguishes the present work from the recent work of Niblett et al [13] where only water drainage was considered in the PTL. The reader will note that Eq. (3) is consistent-with the so-called transferred-substance-state (T-state) formulation first formulated by Spalding [14] for both single-phase and multi-phase chemically-reacting mass transfer problems, as are found in catalytic converters, stirred tanks, and numerous other process engineering applications and equipment. The interested reader can find a discussion of the subject in Beale et al. [15]. At the channel and PTL walls, as well as on the individual fibres, the static contact angle was fixed, as prescribed in Table III. For the initial fields, in the channel $\boldsymbol{U} = U_{in}\hat{\boldsymbol{i}}$, $\alpha_l = 0$ whereas in the PTL $\boldsymbol{U} = U_{el}\hat{\boldsymbol{j}}$, and a value of $\alpha_l = 0.5$ were selected. The matter is discussed further, below.

TABLE III. Boundary conditions.

Description	Symbol	Value
Inlet mixture velocity	U_{in}	10 m/s
Electrode mixture velocity	U_{el}	0.1 m/s
Inlet liquid volume fraction	α_l	0
Electrode liquid volume fraction	α_{el}	9
PTL fibre contact angle	θ_f	150°
PTL box contact angle	θ_w	150°
Gas channel base contact angle	θ_b	150°
Gas channel top and sides contact angle	θ_{ts}	150°

Code and implementation

The open source library OpenFOAM version 7 was employed to obtain solutions to the problem described above.

Results

The results, in terms of droplet formation, are shown in Figs. 3. It can be seen that following an initial transient, the drops are shed from the PTL into the channel, in a fairly regular manner, with some randomness. Fig. 4(a) shows spot values of water volume fraction, α_w, point P, Fig. 1, as a function of time. Figure 4(b) displays similar values of pressure, p (Pa). It can be seen that the pressure rises and falls as liquid droplets pass through point P.

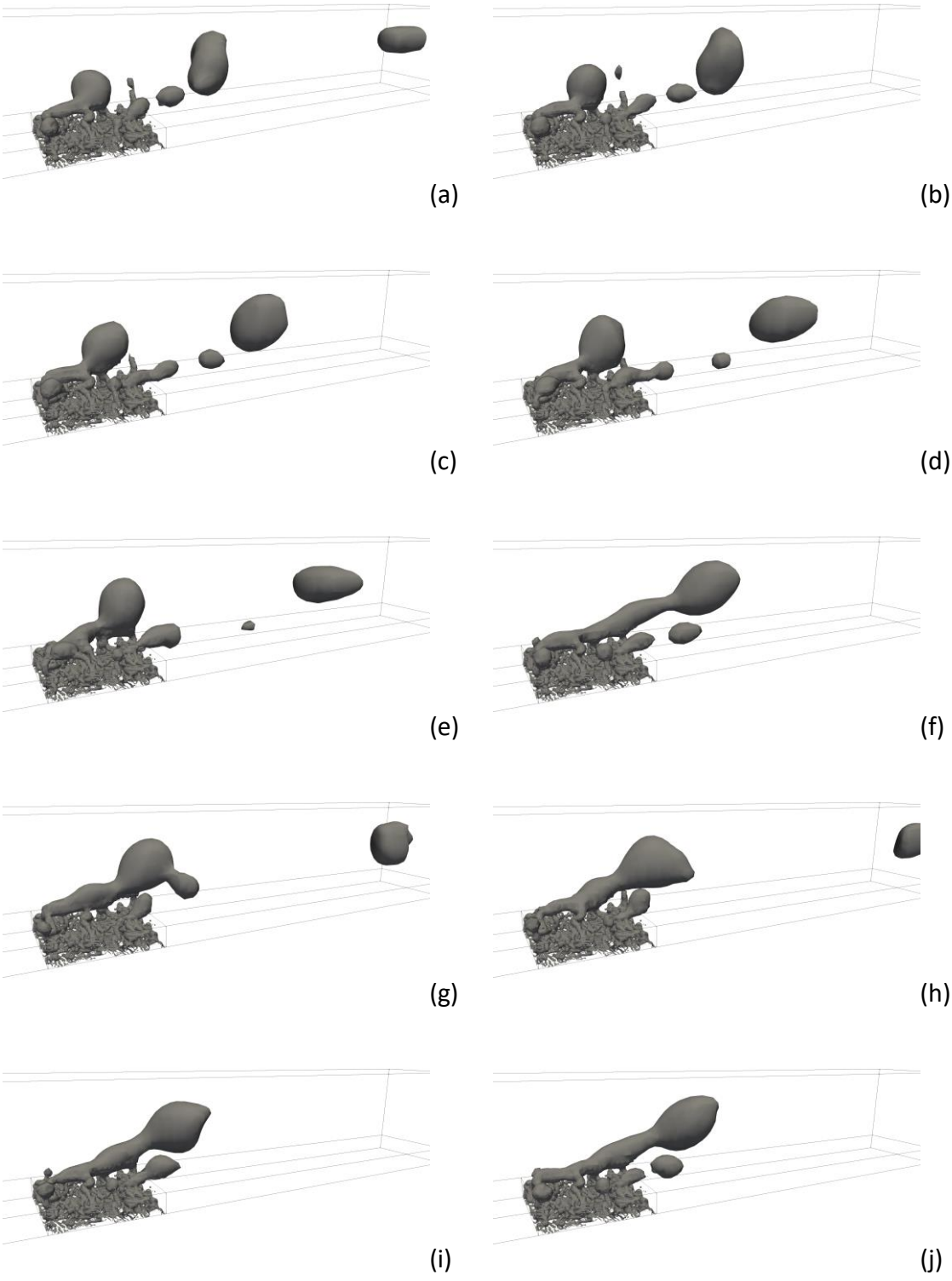

Figure 3. Isosurfaces corresponding to $\alpha_w = 0.5$ at t = (a) 0.0029, (b) 0.0030, (c) 0.0031, (d) 0.0032, (e) 0.0033, (f) 0.0034, (g) 0.0035, (h) 0.0036, (i) 0.0037, (j) 0.0037 sec.

(a) (b)

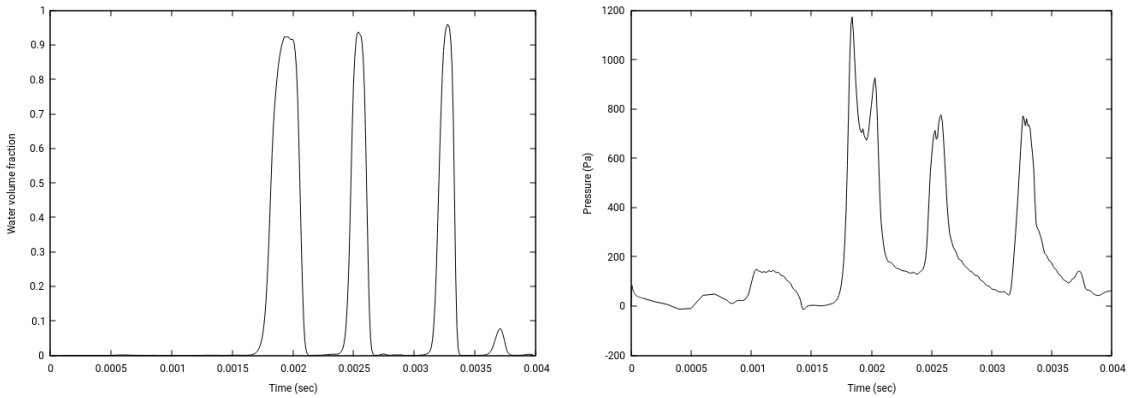

Figure 4. Spot values of (a) water volume fraction, α_w, and (b) pressure , p (Pa) as a function of time, at point P, located in the centre of the gas channel midway between the PTL specimen and the gas outlet.

Discussion

The numerical calculations indicate that though the creation, growth, and subsequent detachment of liquid droplets at the PTL/gas channel interface is reasonably periodic, and yet there is also a certain element of randomness associated with the interactions between the different liquid streams in the PTL-channel interface. This leads to macro-scale fluctuations within the PTL as the drops are formed. However within the majority of the interior of the PTL, towards the electrode, the flow is relatively steady, as indeed would be expected for low Reynolds number flow exhibited in porous media.

The results show that the model is capable, not only of quantifying the two-phase flow of gas and liquid drops, as they are injected into, and convected downstream in the channel by the gas, but also importantly, of dispersing/separating the two-phases within the PTL. Even though the two phases at the electrode boundary are to be considered homogeneous, within the PTL they separate into two heterogeneous liquid and gas phases on (continuum) micro-scale. This separation corresponds to physical reality in that the length scale of the electrochemical reaction at the oxygen electrode of a PEFC is one or two orders of magnitude smaller than the pore sizes in the PTL. This proof-of-concept is exciting as it can lead to series of parametric studies and eventual optimization of the PTL and related micro-porous structures. Some parameters that can be varied include channel-wall and PTL contact angles, and gas and mixture velocities. The T-state prescription for the gas/liquid, Eq. (3) at the electrode may be expressed in a more general form as $\alpha_l = (9+18\beta)/(1+18\beta)$ $\alpha_g = -8/(1+18\beta)$ where β is a net drag coefficient, that is the net number of water molecules dragged to/from the electrode because of protonic drag, back-diffusion, and convection /pressure gradient [16]. Another family of problems amenable to the present analysis are water-electrolyzers which when operated with liquid water as feedstock, generate gas bubbles at the oxygen electrode. Such studies could be useful in identifying multi-phase flow regime changes as a function of gas flow velocity and current density.

Numerical issues

The code consumed numerous weeks of time running in parallel (48 cores). This results from the requirement to keep the Courant number, Co < 1, due to the fact that pore sizes are very small in the PTL. The choice of initial α-fields is important from a convergence perspective: The heterogeneous reaction can only physically take places if both oxygen and water (and also protons) are simultaneously present at the electrode-PTL boundary. The prescriptions $\alpha_l = 1$ (full-wet) or $\alpha_l = 0$ (empty-dry) at t = 0 within the PTL, may be problematic: Although the T-state α-boundary condition will correctly drive interior α-values to equilibrium values, in the range $0 < \alpha < 1$, there is no guarantee that during the initial transient, interior values outside these limits, could arise. If the solver then imposes the limits on the α solution field, as is common, then divergence may arise, and it is recommended that these initial conditions be avoided for the problem-at-hand.

Conclusions

The volume-of-fluid method has successfully been applied to two-phase liquid-gas counter-flow in a PTL, with associated co-flow in the gas channel. The inlet/outlet boundary condition for the homogeneous gas/liquid preduction/destruction at the electrode led to a physically reasonable solution both in the PTL and in the channel.

Future work

The properties of oxygen and water were selected for the two phases considered here, i.e. two-phases each composed of a single species. In fact, for a fuel cell, the composition of atmospheric air varies as oxygen is consumed, $\rho_g = \rho_g\left(y_{O_2}, y_{N_2}, ...\right)$. Therefore conservation of species would add an additional scalar equation for multi-phase multi-species formulation. Moreover, as discussed by Gurau et al., phase change issues, in the form of evaporation/condensation mass transfer are important and lead to water vapor being present in the gas phase. Calculation of inter-phase mass transfer requires the latent heat of evaporation/condensation based on the inter-phase temperature gradients be prescribed. Hence the energy equation and individual species continuity equations should also be solved.

The relatively coarse mesh generated, based on castellated octree refining, was deliberately employed to obtain solutions on a reasonably orthogonal framework. In the future, superior meshes employing surface snapping, and layer insertion will be constructed. These will rapidly increase the mesh size with the potential for further reducing the Courant limit. Mesh adaptation may also prove to be useful. A balance needs to be struck between mesh independence and available computational capabilities. This was always true, however resources were more scarce in the past than now. Indeed massively parallel computers may eventually allow for the PTL region to extend the entire length of the channel, at least for reasonably short channels. In this manner, water management, an important topic in PEFC technology can be improved by detailed mathematical modelling on a micro-scale.

Acknowledgements

The authors wish to thank Mr. Eugen Hoppe for constructing a stereolithography file of the porous material used in this study. Discussions with Prof. Bedii Özdemir on the subject matter of the paper and computational issues, were constructive. Calculations were performed on the high performance computing hardware of the Jülich Aachen Research Alliance (JARA), under grant number JARA0070.

References

1. C. W. Hirt and B. D. Nichols, *J. Comput. Phys.*, **39**(1) 201-225 (1981).
2. F. H. Harlow and A. A. Amsden, *J. Comput. Phys.*, **8**(2) 197-213 (1971).
3. C. T. Crowe, M. P. Sharma, and D. E. Stock, (1977).
4. C. Wang and P. Cheng, *Int J Heat Mass Tran*, **39**(17) 3607-3618 (1996).
5. C. Wang and P. Cheng, *Advances in heat transfer*, **30** 93-196 (1997).
6. V. Gurau, T. A. Zawodzinski, and J. A. Mann, *J. Fuel Cell Sci. Technol.*, **5**(2) 021009 (2008).
7. D. B. Spalding, Numerical Computation of Multi-phase Flow and Heat Transfer, in *Recent Advances in Numerical Methods in Fluids*, C. Taylor, Editor. 1980, Pineridge Press: Swansea. 139-167.
8. A. D. Le and B. Zhou, *J. Power Sources*, **182**(1) 197-222 (2008).
9. M. Andersson, S. B. Beale, U. Reimer, W. Lehnert, and D. Stolten, *Int. J. Hydrogen Energy*, **43**(5) 2961-2976 (2018).
10. M. Andersson, et al., *J. Power Sources*, **404** 159-171 (2018).
11. M. Andersson, S. B. Beale, and W. Lehnert, *eTransportation*, **1** 100003 (2019).
12. M. Andersson, et al., *Int. J. Hydrogen Energy*, **44**(21) 11088-11096 (2019).
13. D. Niblett, A. Mularczyk, V. Niasar, J. Eller, and S. Holmes, *J. Power Sources*, **471** 228427 (2020).
14. D. B. Spalding, *Int J Heat Mass Tran*, **1** 192-207 (1960).
15. S. B. Beale, et al., Heat and mass transfer in fuel cells and stacks, in *"50 Years of CFD in Engineering Sciences" A Commemorative Volume in Honour of D. Brian Spalding*, A.K. Runchal, Editor. 2020, Springer.
16. S. B. Beale, *Int. J. Hydrogen Energy*, **40**(35) 11641-11650 (2015).